



eISSN: 2321-323X
pISSN: 2395-0781

Research Article

A comparative molecular dynamics study of MurA enzymes from *E. coli* and *M. tuberculosis*

Shahzaib Ahamad¹, Faez Iqbal Khan^{2,*}, Urmil Bajpai³, Shahnawaz Ali⁴, Neeraja Dwivedi¹ and Md. Imtaiyaz Hassan⁴

¹Department of Biotechnology, College of Engineering & Technology, IFTM University, Moradabad, India.

² Department of Chemistry, Durban University of Technology, Durban-4000, South Africa.

³ Department of Biomedical Sciences, Acharya Narendra Dev College, University of Delhi, India.

⁴ Centre for Interdisciplinary Research in Basic Sciences, Jamia Millia Islamia, New Delhi, India.

Abstract

UDP-N-acetylglucosamine 1-carboxyvinyltransferase (MurA) is an initial step enzyme, involved in the synthesis of major structural elements (Murein) of bacterial cell wall. MurA shows a similar structural pattern as compared to 5-enolpyruvylshikimate-3-phosphate (EPSP) synthase consisting of two domains encasing catalytic cleft between them. Since crystal structure of *Mycobacterium tuberculosis* (*Mtb*-MurA) is not available; therefore, we predicted the three-dimensional (3D) structure using homology modeling approach to understand its detailed structural features. The molecular dynamics (MD) simulations of MurA enzymes from *Mycobacterium tuberculosis* and *Escherichia coli* revealed valuable insights into the folding pattern. MD simulation of the *E. coli*-MurA and the predicted *Mtb*-MurA showed similar trajectories and folding patterns. The MurA enzymes remained in their compact and stable state during the 20 ns simulations.

Keywords: MurA enzyme; MD simulation; Homology modeling; Molecular docking; *E. coli*; Protein structure prediction

Abbreviations: RMSD, Root Mean Square Deviation; MD, Molecular dynamics; GROMACS, GROningen MACHine for Chemical Simulations; OPLS-AA/L, Optimized Potential for Liquid Simulations/ all atoms; SASA, solvent accessible surface area; PDB, Protein Data Bank.

***Corresponding author:** Faez Iqbal Khan, Department of Chemistry, Faculty of Applied Science, Durban University of Technology, Durban 4000, South Africa E- mail: khanfaeziqbal@gmail.com

1. Introduction

Bacterial cell wall structure and its composition are two essential features required for its survival and growth inside the host [1]. Cell wall is considered as a major target to most of the antibiotics [2]. Murein is a major structural element of the bacterial cell wall formed by the activity of UDP-N-acetylglucosamine 1-carboxyvinyltransferase (MurA, EC 2.5.1.7) enzyme [3]. Murein synthesis is initiated by the transfer of

enolpyruvylgroup from phosphoenolpyruvate (pyruvate-P) to the 3-hydroxyl of UDP-N-acetylglucosamine (UDP-GlcNAc) [4]. *Escherichia coli* MurA (*E. coli*-MurA) behaves as a potential target for the broad spectrum antibiotic like fosfomycin [5]. MurA is the first enzyme in the synthesis of bacterial cell wall [6]. In a similar way 5-enolpyruvylshikimate-3-phosphate (EPSP) synthase (EC 2.5.1.19) also catalyze a similar reaction and is the sixth enzyme in the shikimate pathway [7]. In contrast to the irreversible inhibition of MurA

by fosfomycin, glyphosate reversibly binds to the EPSP synthase [7]. Fosfomycin attaches irreversibly to the thiol group of MurA cysteine residue obtained from *E. coli* and *E. cloacae* [8, 9]. Moreover, it was found that the inactivation of MurA (*E. coli*) by fosfomycin was reported to be reversible followed by covalent modification [9].

Mycobacterium tuberculosis MurA (*Mtb*-MurA) is an attractive target for small molecule inhibitors with the potential to have broad antibacterial activity [10]. The structure of *Mtb*-MurA consists of two domains, similar to the protein architecture of EPSP synthase [6]. In contrast to the available structure information, a little is known about the dynamics of *E. coli*-MurA as well as *Mtb*-MurA. 3D model of *Mtb*-MurA was predicted by homology modeling methods in order to understand structure and conformation patterns [11]. In the absence of experimental data, model building on the basis of a known 3D structure of a homologous protein is at present the only reliable method to obtain the structural information [12]. The main objective behind homology modeling is to ensure overall quality of the models, accuracy of prediction and evaluating the parameters provided by the various tools. Homology modeling is widely used in structure-based drug discovery [13-19]. Homology modeling can be employed to study the effect of mutations on the protein structure, active site prediction, designing novel drugs, and to study folding patterns using molecular dynamics (MD) simulations [20-22].

In order to understand the factors contributing to its folding and stability, we performed MD simulations in explicit water environment at temperature of 300 K to provide a deeper insight into the structural features of both the enzymes [23]. MD simulations of MurA enzymes provided detailed information on the fluctuations and conformational changes. These methods are used to investigate the dynamics behaviours of biological molecules [20, 21]. MD simulations can track system behaviour and understanding of protein folding [24, 25]. In explicit conditions, all atoms of a protein and surrounding water molecules move in a series of time steps. At each time step, the forces on each atom, the atomic positions and the velocities are computed [26]. The observed

comparative study suggested that *E.coli*-MurA and *Mtb*-MurA shows similar trajectories pattern in its structural framework.

2. Materials and methods

Structure prediction and evaluation

3D structure of *Mtb*-MurA was predicted using homology method. The structural homolog search was performed in the Protein Data Bank (PDB) [27] using PSI-BLAST, HHpred [28], HMMER [29] and Phyre [30]. A BLAST [31] search with identity >30% was considered as the suitable template for the structure prediction [20, 24]. The HHpred identified structural homologue in the PDB, structural classification of proteins (SCOP) and CATH. The fold recognition methods were used to optimize the sequence-structure alignment, which was further utilized to develop the three dimensional models using MODELLER [32]. The homology modeling is based on the alignments of the studied proteins. The most reliable model was evaluated on the basis of root mean square deviation (RMSD) and TM score [25]. The selected models were further refined using SCWRL 4.0 [33] and CHARMM [34] energy minimization. The GROMOS [35] algorithm implemented in DeepView [36] was used for energy minimization of the predicted models. The 3D models were evaluated using PROCHECK and ERRAT server [37, 38].

Molecular dynamic simulation

MD simulation method was performed at the molecular mechanics level implemented in the GROMACS 4.6.5 computer program [39] using the all atom functions by OPLS (optimized potential for liquid simulation) on *Mycobacterium* MurA (*Mtb*-MurA) and *E.coli* MurA (*E.coli*-MurA) at 300 K in order to investigate and compare the folding profile [40]. Both the proteins were first soaked in a cubic box of water molecules with a dimension of 10 Å. The editconf and genbox modules were used for creating boundary conditions and solvation respectively. The spc216 template was used to solvate the proteins. The charges on the proteins were neutralized by the addition of Na⁺ and Cl⁻ ions to maintain neutrality. The system was then minimized using 1500 steps of steepest descent. The temperature of the

systems was raised from 0 to 300 K during their equilibration period (100 ps) under periodic boundary conditions. Equilibration was performed in two phases of NVT ensemble (constant number of particles, volume, and temperature at 100 ps) and NPT ensemble (constant number of particles, pressure, and temperature at 100 ps). After the equilibration phase, the particle-mesh Ewald method [41] was applied and the production phases consisting of 20 ns were performed. The resulting trajectories were analysed using *g_energy*, *g_gyrate*, *g_rms*, *g_rmsf*, *g_hbond* and *g_sas* utilities of GROMACS. All the graphic presentations of the 3D model were prepared using VMD (Visual Molecular Dynamics) [42].

3. Results and discussion

Structure analysis

The sequence of *Mtb*-MurA was obtained from tuberculist database (Uniprot: P0A5L2). The Molecular mass of *Mtb*-MurA was 44-kDa with the isoelectric point of 5.3. The HHpred and PSI-Blast identifies *Bacillus Anthracis*, *Pseudomonas Aeruginosa*, *Listeria*

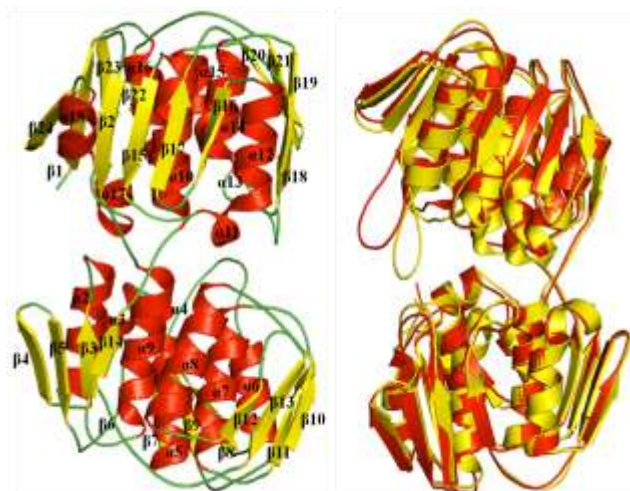


Fig.1: (A) 3D structure *Mtb*-MurA with 18 α -helices, and 24 β -sheets. (B) Overlaid structures of model and template. Unaligned regions are clearly indicated in the structure.

Monocytogenes, and *E. coli* MurA as templates with > 45% identity. The *E. coli* MurA (PDB Id: 3KR6) was selected as a suitable template for the structure prediction of *Mtb*-MurA. The MODELLER aligned the template structure and query sequence and finally generated the 3-D

models by satisfying the spatial restraints [43]. The predicted structures showed low violations of restraints are considered to be more precise as shown in Fig. 1A.

Subsequently, 5 models were generated and evaluated on the basis of RMSD and TM-score. The predicted model showed similar architecture with other MurA enzymes in its framework. is highlighting the overhanging sequence which is further modeled using *ab initio* protocol of the I-TASSER [44]. The generated model was optimized using the CHARMM 22 force field present in the DS. The side chains of the model were refined using the SCWRL4 package [45]. Then the energy minimization of the 3-D structure was performed in order to avoid bad molecular contacts by using the Deepview that contain steepest descent protocol implemented in GROMOS. The minimized energy for the optimized models of *Mtb*-MurA was observed to be -18543.44 kJ/mol. The RMSD was found to be 0.613 between the template and initial predicted model structure of *Mtb*-MurA indicating similar conformations (Fig. 1B). Procheck showed 97.3% of the residues are in the allowed region of the Ramachandran plot [46]. The overall quality factor score predicted by Errat was 96.6 for *Mtb*-MurA.

The topology for the given structure of *Mtb*-MurA was generated using PDBsum, in order to understand the detailed structural features of the structure [47]. The initial *Mtb*-MurA structure contains strands 25.6% (107 aa), alpha helix 31.8 (133 aa) and 3-10 helix 10 % (2.4 aa). The structure showed the presence of 6 beta sheets, 4 beta-alpha-beta motifs, 5 β -hairpins, 2 β -bulge, 24 β -strands, 17 α -helices, 32 helix-helix interaction, 21 β -turns and 8 γ -turns. Moreover, there was no disulphide bonds were found in the structure of *Mtb*-MurA (Fig. 2).

Systems stability during simulations

MD simulations of *Mtb*-MurA showed an acceptable stability profile at a temperature of 300 K. To ascertain the equilibration of the systems prior to MD analysis, the average total energy, potential energy and the constant average fluctuation of temperatures were monitored. The constant temperature fluctuations at 300 K on both the *Mtb*-MurA and

Ecoli-MurA suggested a stable and accurate nature of the MD simulations performed (Fig. 3). The average potential energy and total energy of *E.coli-MurA* were found to be -1237662.367 kJ/mol and -1045427.775 kJ/mol, while for *Mtb-MurA* were \square 1198225.041kJ/mol and \square 1012307.599 kJ/mol, respectively. The structure of *Mtb-MurA* showed comparable average energies values suggesting the stable conformation of predicted *Mtb-MurA* structure.

Radius of gyration

Radius of gyration (Rg) is a parameter linked to

than *Ecoli-MurA* during simulations. The overall Rg values were found to be in the range of 2.18-2.20 nm for both the proteins. The result clearly suggests that the MurA enzymes of both *E. coli* and *M. tuberculosis* showed similar compactness at 300 K (Fig. 4).

Root mean square deviations

Root mean square deviation (RMSD) is one of the most important fundamental properties to establish whether the protein is stable and close to the experimental structure [47, 48]. RMSD is a measure of the deviation of the

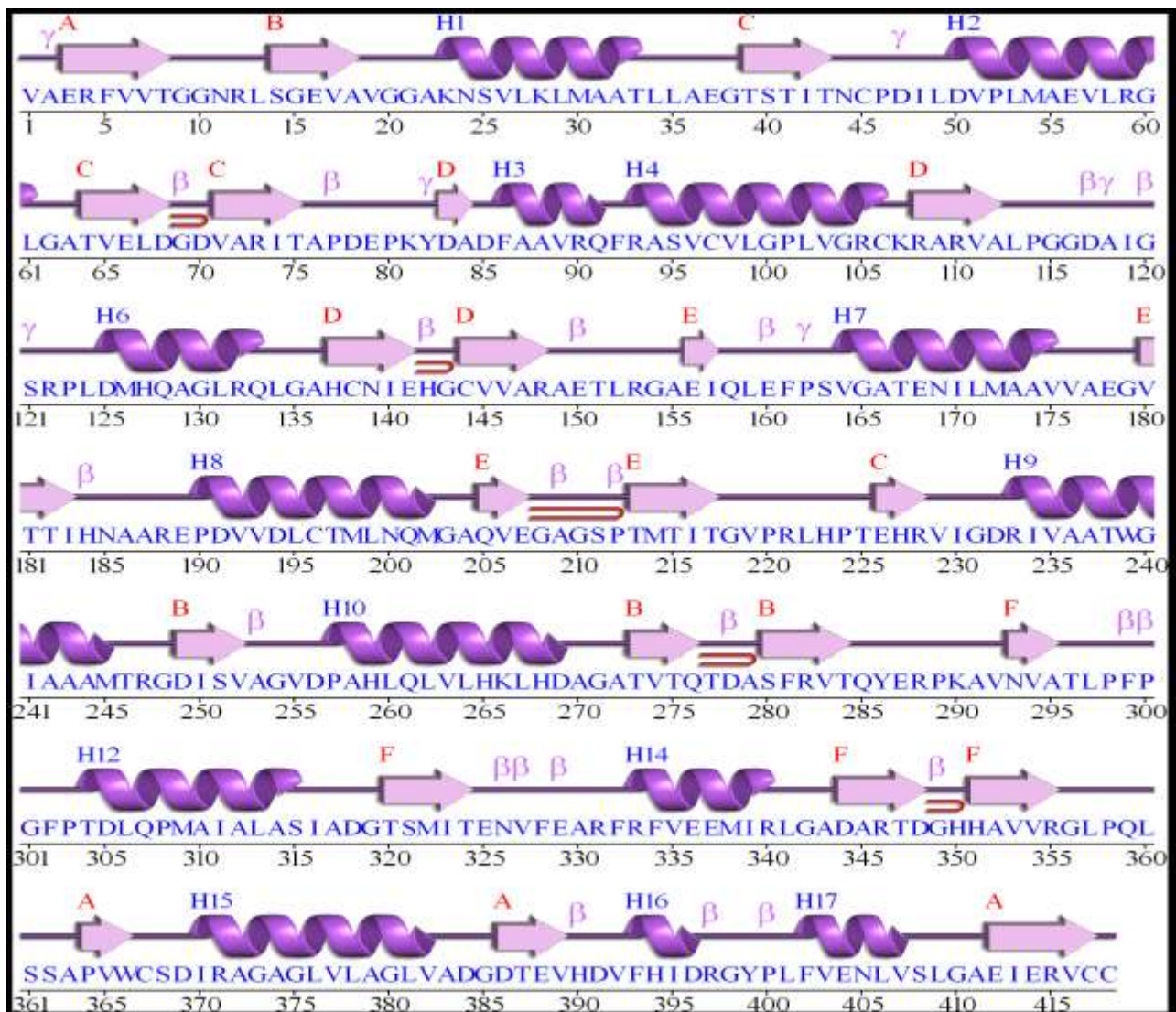


Fig. 2: The topology map of Mtb-MurA protein generated by PDBsum showing secondary structure elements in the framework

the tertiary structural volume of a protein and has been applied to obtain insight into the stability of the protein in a biological system along the MD simulation. The average Rg for *Mtb-MurA* structures was found to be lower

conformational stability of the proteins from the backbone structure to the initial starting structure. The *E. coli-MurA* and *Mtb-MurA* showed constant RMS deviations (0.15-0.175 nm) from the initial structure throughout the 20

ns time scales (Fig. 5). The behaviour of *Mtb*-MurA in the explicit solvent conditions was related to that of *E. coli*-MurA. This suggested that the predicted structure of *Mtb*-MurA is a structural homologue to that of *E. coli*-MurA, thus indicating the reliability of predicted structure.

Root of mean square fluctuation

Vibrations around the equilibrium are not random, but depend on the local structure flexibility. To calculate the average fluctuation of all residues during the simulation, the root mean square fluctuation (RMSF) of the C α atoms of protein from the primary structure were plotted as a function of residue number using *g_rmsf* module of GROMACS [48]. The RMSF of *Mtb*-MurA as a function of amino acid residues was calculated and compared with *E. coli*-MurA during the simulations. A similar pattern of RMSF was observed for both the proteins (Fig. 6). While, a slightly different pattern was observed in the β -hairpin region present between 260-280 amino acid residues.

Hydrogen-bond formation

Due to the lack of a high resolution protein structure, structural analyses of H-bonds were not very conclusive. The hydrogen bonds

formed between the amino acid residues of the protein controls the protein structure conformation and the presence of extra hydrogen bonds renders the protein structure more resistant to unfolding [49]. The helix forming residues are thought to be a major contributing factor for thermostability. The hydrogen-bonds between *Mtb*-MurA and water molecules were calculated and it was found to be slightly less than the *E. coli*-MurA (Fig. 7).

Solvent accessible surface area

Solvent accessible surface area (SASA) is defined as the surface area of a protein which interacts with its solvent molecules.

Denaturation of protein causes increase in SASA due to the hydrophobic regions exposed to solvent during unfolding [50,51]. The calculated SASA values for *Mtb*-MurA with respect to backbone were found to be exactly similar to *E. coli*-MurA at 300 K (Fig. 8) suggesting that the hydrophobic residues present in the *Mtb*-MurA molecule are not exposed to the solvent i.e. the proteins remained in its folded form. It is suggested that the predicted accessible surface area can be used to improve prediction of protein secondary structure.

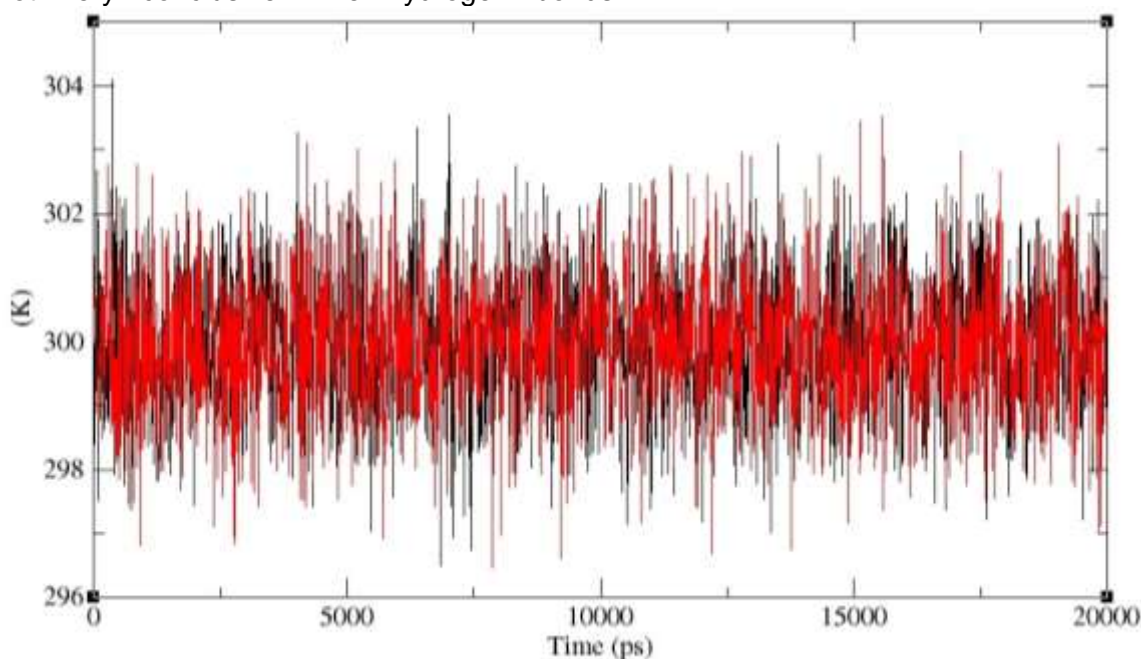


Fig. 3: The average temperature fluctuations as a function of time obtained at 300 K. Black and red colour represent values obtained for *E. coli*-MurA and *Mtb*-MurA, respectively.

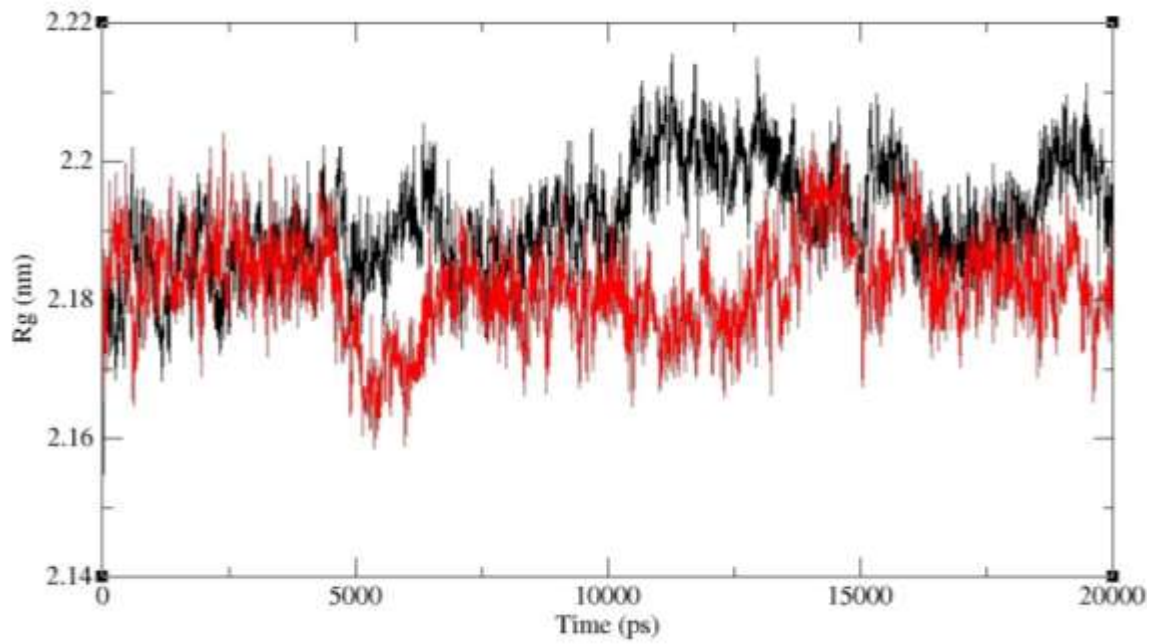


Fig. 4: The radius of gyration values as a function of time obtained at 300 K. Values were calculated with the use of C^α atoms. Black and red colour represents values obtained for *E. coli*-MurA and *Mtb*-MurA, respectively.

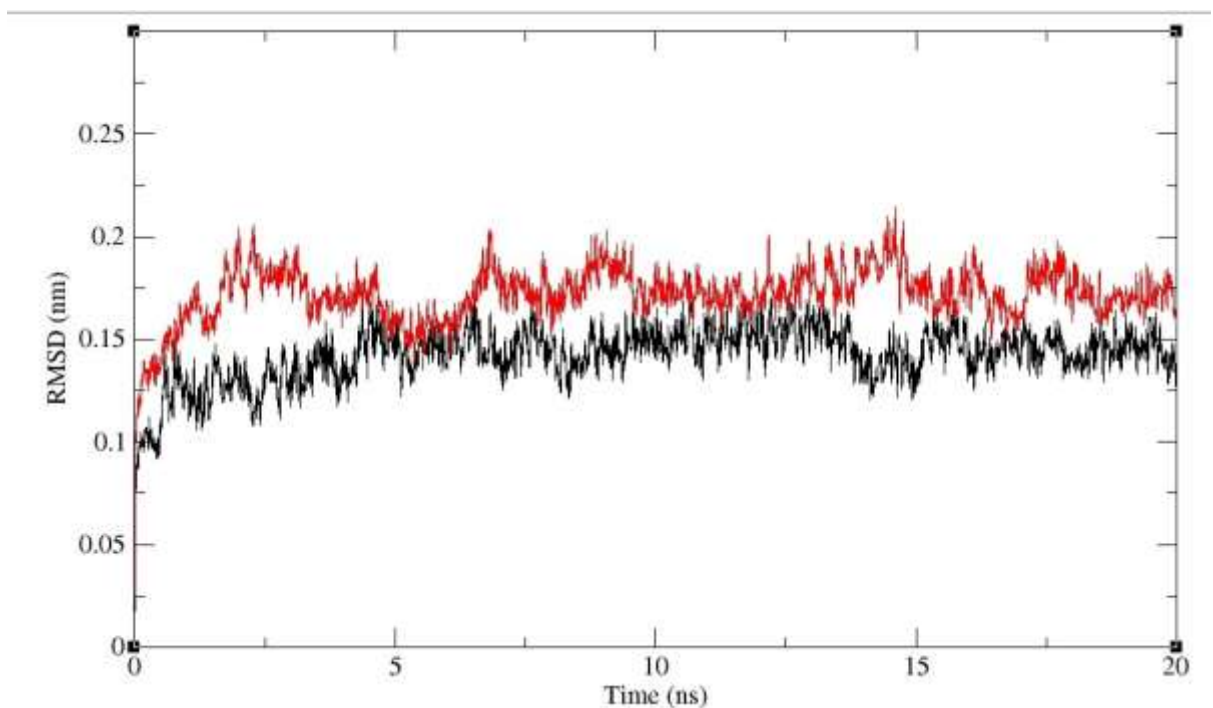


Fig. 5: RMS deviation values as a function of time obtained at 300 K. Values were calculated with the use of C α atoms. Black and red colour represent values obtained for *E. coli*-MurA and *Mtb*-MurA, respectively.

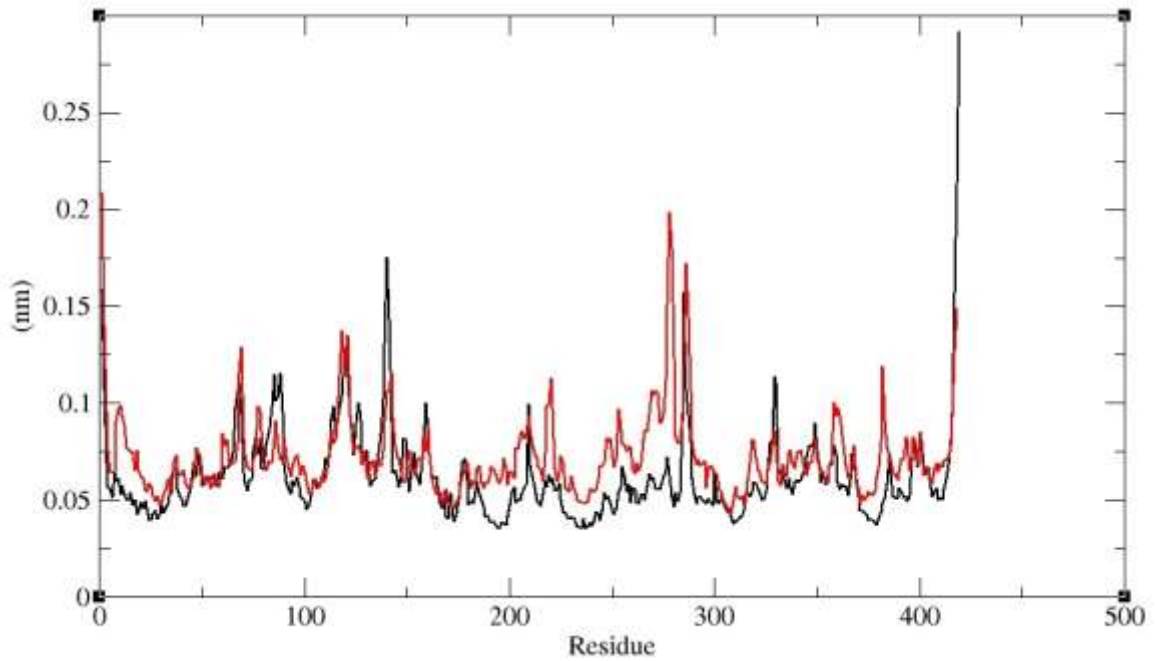


Fig. 6: Average RMSF as a function of amino acid sequence numbers at 300 K. Values were calculated with the use of C^α atoms. Black and red colour represent values obtained for *E. coli*-MurA and *Mtb*-MurA, respectively.

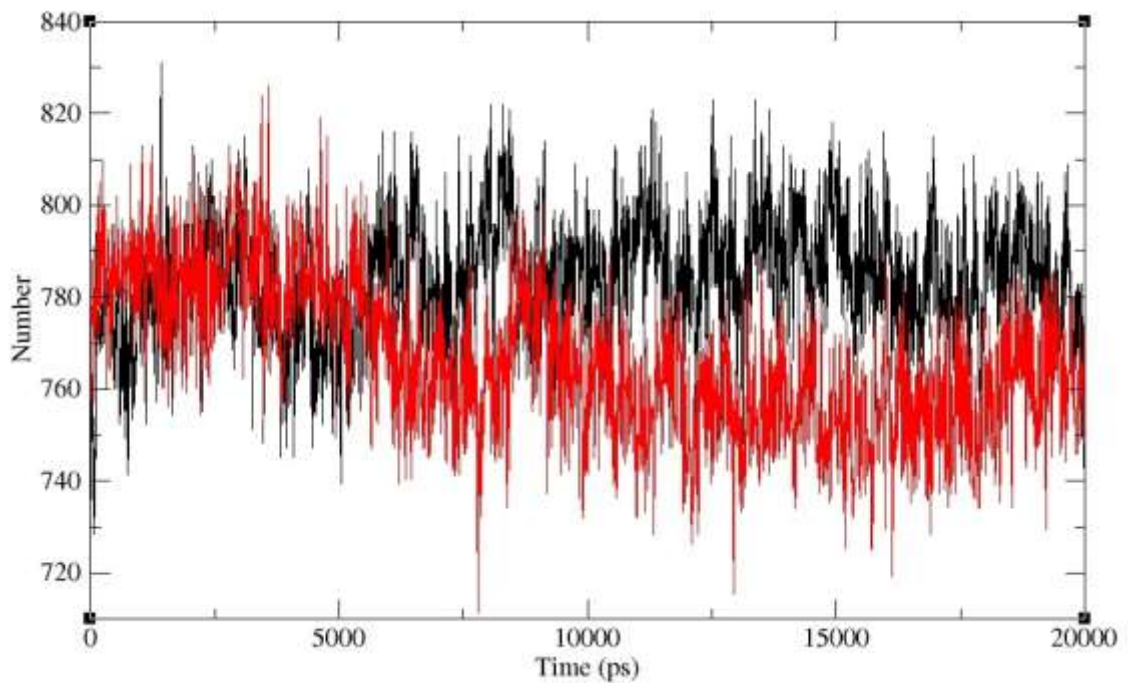


Fig. 7: Average number of hydrogen bonds between protein and water as a function of time obtained at 300 K. Black and red colour represent values obtained for *E. coli*-MurA and *Mtb*-MurA, respectively.

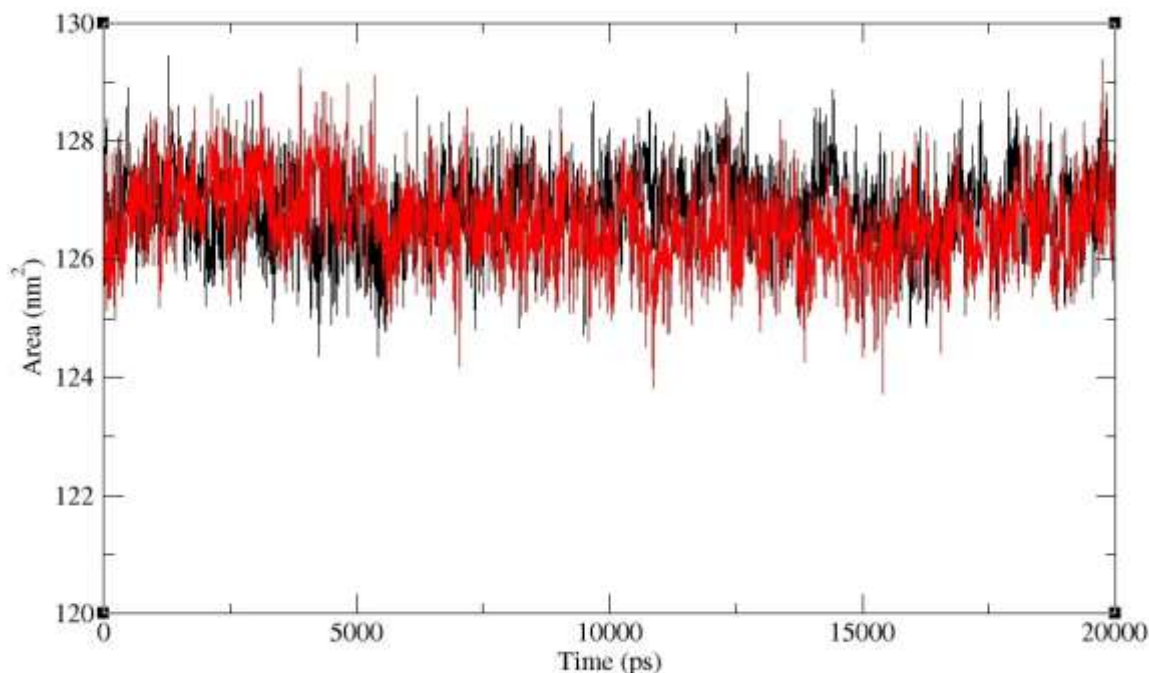


Fig. 8: Solvent Accessible Surface Area (SASA) as a function of time. Values were calculated with the use of C^α atoms. Black and red colour represents values obtained for *E. coli*-MurA and *Mtb*-MurA, respectively.

Conclusions

MurA enzyme is a potential target for broad spectrum antibiotic for MDR-TB. It is essentially involved in making the cell intact inside host by synthesizing Murein. MurA provides structural stability to organism. In this study, 3D structure of *Mtb*-MurA was generated with a high precision refinement to understand its structural features. A 20 ns MD simulations were performed in a box of water molecules to understand the behaviour of *E. coli*-MurA and *Mtb*-MurA. The results suggested that the compactness and the stability of *Mtb*-MurA were similar to that of *E. coli*-MurA. Both enzymes showed similar trajectories in the solvent molecules.

Acknowledgments

The authors would like to express our gratitude to the Centre for high performance computing, an initiative support by the Department of Science and Technology of South Africa.

Conflict of Interest

The authors have no substantial financial or commercial conflicts of interest with the current work or its publication.

References

- [1] Silhavy, T.J., D. Kahne, and S. Walker, *The bacterial cell envelope*. Cold Spring Harb Perspect Biol, 2010. 2(5): p. a000414.
- [2] Vollmer, W. and U. Bertsche, *Murein (peptidoglycan) structure, architecture and biosynthesis in Escherichia coli*. Biochim Biophys Acta, 2008. 1778(9): p. 1714-34.
- [3] Vesic, D. and C.J. Kristich, *MurAA is required for intrinsic cephalosporin resistance of Enterococcus faecalis*. Antimicrob Agents Chemother, 2012. 56(5): p. 2443-51.
- [4] Mengin-Lecreulx, D. and J. van Heijenoort, *Copurification of glucosamine-1-phosphate acetyltransferase and N-acetylglucosamine-1-phosphate uridyltransferase activities of Escherichia coli: characterization of the glmU gene product as a bifunctional enzyme catalyzing two subsequent steps in the pathway for UDP-N-acetylglucosamine synthesis*. J Bacteriol, 1994. 176(18): p. 5788-95.
- [5] Shahab, M., et al., *Cloning, expression and characterization of UDP-N-acetylglucosamine enolpyruvyl transferase (MurA) from Wolbachia endosymbiont of human lymphatic filarial*

- parasite *Brugia malayi*. *PLoS One*, 2014. 9(6): p. e99884.
- [6] Skarzynski, T., et al., *Structure of UDP-N-acetylglucosamine enolpyruvyl transferase, an enzyme essential for the synthesis of bacterial peptidoglycan, complexed with substrate UDP-N-acetylglucosamine and the drug fosfomycin*. *Structure*, 1996. 4(12): p. 1465-74.
- [7] Steinrucken, H.C. and N. Amrhein, *The herbicide glyphosate is a potent inhibitor of 5-enolpyruvyl-shikimic acid-3-phosphate synthase*. *Biochem Biophys Res Commun*, 1980. 94(4): p. 1207-12.
- [8] Wanke, C. and N. Amrhein, *Evidence that the reaction of the UDP-N-acetylglucosamine 1-carboxyvinyltransferase proceeds through the O-phosphothioketal of pyruvic acid bound to Cys115 of the enzyme*. *Eur J Biochem*, 1993. 218(3): p. 861-70.
- [9] Brown, E.D., et al., *Detection and characterization of a phospholactoyl-enzyme adduct in the reaction catalyzed by UDP-N-acetylglucosamine enolpyruvyl transferase, MurZ*. *Biochemistry*, 1994. 33(35): p. 10638-45.
- [10] Silver, L.L., *Challenges of antibacterial discovery*. *Clin Microbiol Rev*, 2011. 24(1): p. 71-109.
- [11] Sali, A. and T.L. Blundell, *Comparative protein modelling by satisfaction of spatial restraints*. *J Mol Biol*, 1993. 234(3): p. 779-815.
- [12] Vyas, V.K., et al., *Homology modeling a fast tool for drug discovery: current perspectives*. *Indian J Pharm Sci*, 2012. 74(1): p. 1-17.
- [13] Hassan, I., *Recent Advances in the Structure-based Drug design (SBDD) and Discovery*. *Curr Top Med Chem*, 2015.
- [14] Hassan, M.I., A. Aijaz, and F. Ahmad, *Structural and functional analysis of human prostatic acid phosphatase*. *Expert Rev Anticancer Ther*, 2010. 10(7): p. 1055-68.
- [15] Hassan, M.I., et al., *Structure-guided design of peptidic ligand for human prostate specific antigen*. *J Pept Sci*, 2007. 13(12): p. 849-55.
- [16] Hassan, M.I., A. Saxena, and F. Ahmad, *Structure and function of von Willebrand factor*. *Blood Coagul Fibrinolysis*, 2012. 23(1): p. 11-22.
- [17] Hassan, M.I., A. Toor, and F. Ahmad, *Progastriscin: structure, function, and its role in tumor progression*. *J Mol Cell Biol*, 2010. 2(3): p. 118-27.
- [18] Thakur, P.K. and I. Hassan, *Discovering a potent small molecule inhibitor for gankyrin using de novo drug design approach*. *Int J Comput Biol Drug Des*, 2011. 4(4): p. 373-86.
- [19] Thakur, P.K., et al., *Search of potential inhibitor against New Delhi metallo-beta-lactamase 1 from a series of antibacterial natural compounds*. *J Nat Sci Biol Med*, 2013. 4(1): p. 51-6.
- [20] Khan, F.I., et al., *Thermostable chitinase II from *Thermomyces lanuginosus* SSBP: Cloning, structure prediction and molecular dynamics simulations*. *J Theor Biol*, 2015. 374: p. 107-14.
- [21] Stephens, D.E., et al., *Creation of thermostable and alkaline stable xylanase variants by DNA shuffling*. *J Biotechnol*, 2014. 187: p. 139-46.
- [22] Khan, F.I., et al., *Large scale analysis of the mutational landscape in beta-glucuronidase: A major player of mucopolysaccharidosis type VII*. *Gene*, 2015.
- [23] Kony, D.B., P.H. Hunenberger, and W.F. van Gunsteren, *Molecular dynamics simulations of the native and partially folded states of ubiquitin: influence of methanol cosolvent, pH, and temperature on the protein structure and dynamics*. *Protein Sci*, 2007. 16(6): p. 1101-18.
- [24] Gramany, V., et al., *Cloning, expression and molecular dynamics simulations of a xylosidase obtained from *Thermomyces lanuginosus**. *J Biomol Struct Dyn*, 2015: p. 1-34.
- [25] Anwer, K., et al., *Role of N-terminal residues on folding and stability of C-phycoerythrin: simulation and urea-induced denaturation studies*. *J Biomol Struct Dyn*, 2015. 33(1): p. 121-33.
- [26] Borhani, D.W. and D.E. Shaw, *The future of molecular dynamics simulations in drug discovery*. *J Comput Aided Mol Des*, 2012. 26(1): p. 15-26.
- [27] Berman, H.M., et al., *The Protein Data Bank*. *Nucleic Acids Res*, 2000. 28(1): p. 235-42.
- [28] Soding, J., A. Biegert, and A.N. Lupas, *The HHpred interactive server for protein homology detection and structure prediction*. *Nucleic Acids Res*, 2005. 33(Web Server issue): p. W244-8.
- [29] Finn, R.D., J. Clements, and S.R. Eddy, *HMMER web server: interactive sequence similarity searching*. *Nucleic Acids Res*, 2011. 39(Web Server issue): p. W29-37.
- [30] Kelley, L.A. and M.J. Sternberg, *Protein structure prediction on the Web: a case study using the Phyre server*. *Nat Protoc*, 2009. 4(3): p. 363-71.
- [31] Altschul, S.F., et al., *Basic local alignment search tool*. *J Mol Biol*, 1990. 215(3): p. 403-10.
- [32] Eswar, N., et al., *Protein structure modeling with MODELLER*. *Methods Mol Biol*, 2008. 426: p. 145-59.
- [33] Wang, Q., A.A. Canutescu, and R.L. Dunbrack, Jr., *SCWRL and MolIDE: computer programs for side-chain conformation prediction and homology modeling*. *Nat Protoc*, 2008. 3(12): p. 1832-47.
- [34] Vanommeslaeghe, K., et al., *CHARMM general force field: A force field for drug-like molecules compatible with the CHARMM all-atom additive biological force fields*. *J Comput Chem*, 2010. 31(4): p. 671-90.

- [35] Fraternali, F. and W.F. Van Gunsteren, *An efficient mean solvation force model for use in molecular dynamics simulations of proteins in aqueous solution*. *J Mol Biol*, 1996. 256(5): p. 939-48.
- [36] Kaplan, W. and T.G. Littlejohn, *Swiss-PDB Viewer (Deep View)*. *Brief Bioinform*, 2001. 2(2): p. 195-7.
- [37] Jadaun, A., et al., *In silico screening for novel inhibitors of DNA polymerase III alpha subunit of Mycobacterium tuberculosis (MtbDnaE2, H37Rv)*. *PLoS One*, 2015. 10(3): p. e0119760.
- [38] Singh, R.P., et al., *Structure prediction and analysis of MxaF from obligate, facultative and restricted facultative methylobacterium*. *Bioinformation*, 2012. 8(21): p. 1042-6.
- [39] Van Der Spoel, D., et al., *GROMACS: fast, flexible, and free*. *J Comput Chem*, 2005. 26(16): p. 1701-18.
- [40] Khan, F., et al., *Chitinase from Thermomyces lanuginosus SSBP and its biotechnological applications*. *Extremophiles*, 2015: p. 1-12.
- [41] Norberto de Souza, O. and R.L. Ornstein, *Molecular dynamics simulations of a protein-protein dimer: particle-mesh Ewald electrostatic model yields far superior results to standard cutoff model*. *J Biomol Struct Dyn*, 1999. 16(6): p. 1205-18.
- [42] Humphrey, W., A. Dalke, and K. Schulten, *VMD: visual molecular dynamics*. *J Mol Graph*, 1996. 14(1): p. 33-8, 27-8.
- [43] Eswar, N., et al., *Comparative protein structure modeling using Modeller*. *Curr Protoc Bioinformatics*, 2006. Chapter 5: p. Unit 5 6.
- [44] Roy, A., A. Kucukural, and Y. Zhang, *I-TASSER: a unified platform for automated protein structure and function prediction*. *Nat Protoc*, 2010. 5(4): p. 725-38.
- [45] Krivov, G.G., M.V. Shapovalov, and R.L. Dunbrack, Jr., *Improved prediction of protein side-chain conformations with SCWRL4*. *Proteins*, 2009. 77(4): p. 778-95.
- [46] Ramachandran, G.N., C. Ramakrishnan, and V. Sasisekharan, *Stereochemistry of polypeptide chain configurations*. *J Mol Biol*, 1963. 7: p. 95-9.
- [47] Laskowski, R.A., et al., *PDBsum: a Web-based database of summaries and analyses of all PDB structures*. *Trends Biochem Sci*, 1997. 22(12): p. 488-90.
- [48] Kuzmanic, A. and B. Zagrovic, *Determination of ensemble-average pairwise root mean-square deviation from experimental B-factors*. *Biophys J*, 2010. 98(5): p. 861-71.
- [49] Globus, T., I. Sizov, and B. Gelmont, *Sub-THz specific relaxation times of hydrogen bond oscillations in E.coli thioredoxin*. *Molecular dynamics and statistical analysis*. *Faraday Discuss*, 2014. 171: p. 179-93.
- [50] Ali, S.A., et al., *A review of methods available to estimate solvent-accessible surface areas of soluble proteins in the folded and unfolded states*. *Curr Protein Pept Sci*, 2014. 15(5): p. 456-76.
- [51] Khan, F., et al., *Chitinase from Thermomyces lanuginosus SSBP and its biotechnological applications*. *Extremophiles*, 2015. 19(6): p. 1055-1066.